Dalton Transactions

ROYAL SOCIETY
OF CHEMISTRY

PERSPECTIVE

4,2′:6′,4′′-Terpyridines: diverging and diverse building blocks in coordination polymers and metallomacrocycles

Catherine E. Housecroft

4,2′:6′,4′′-Terpyridine (4,2′:6′,4′′-tpy) is one of the less well documented isomers of the well-established bis-chelating 2,2′:6′,2′′-terpyridine. The N-donors of the outer rings in 4,2′:6′,4′′-tpy subtend an angle of 120°, leading to a description of 4,2′:6′,4′′-tpy as a divergent ligand. Because it typically binds metal ions through the outer N-donors only, 4,2′:6′,4′′-tpy is an ideal linker for combination with metal nodes (often geometrically flexible d^{10} ions) in coordination polymers and metallomacrocyclic complexes. The facile functionalization of terpyridines in the 4′-position allows access to a suite of 4′-X-4,2′:6′,4′′-tpy ligands in which the 4′-substituent, X, can be selected to assist in directing the metal–ligand assembly process. This overview of recent advances in the chemistry of 4,2′:6′,4′′-tpy and its 4′-substituted derivatives looks at relationships within a series of chiral polymers, competition between the formation of metallocyclic complexes *versus* polymers, and the use of extended aryl systems to encourage the formation of coordination polymers in which π-stacking of arene domains dominates in the assembly process. Use of metal(II) acetates is key to the formation of paddle-wheel and larger cluster nodes that direct the assembly of both predetermined and unexpected architectures.

Department of Chemistry, University of Basel, Spitalstrasse 51, CH-4056 Basel, Switzerland. E-mail: catherine.housecroft@unibas.ch

Catherine E. Housecroft

Catherine E. Housecroft is Titular Professor of Chemistry at the University of Basel. She is co-director of a highly active research group with Professor Edwin C. Constable, and has a broad range of interests spanning organometallic and coordination chemistries. Current research is focused towards the application of coordination chemistry to sustainable energy and functional coordination polymers. She has published close to 400 research papers, in addition to many reviews and book chapters. She is an internationally recognized author of undergraduate textbooks: Chemistry *(coauthored with her husband Edwin Constable) and* Inorganic Chemistry *(with Alan Sharpe) are both in their fourth editions.*

Introduction

Ligand design[1] is fundamental to advances in coordination chemistry, and the development of metalloligands[2,3] and 'expanded ligands'[4] has provided the coordination chemist with a toolkit of motifs with which to direct the assembly of large molecular arrays and one-, two- and three-dimensional coordination polymers and networks.[5–7] At this point, it is prudent to note the debate surrounding relevant terminology, *viz.* coordination polymer *versus* metal–organic framework (MOF).[8] In this perspective review, the infinite structures described are termed coordination polymers, irrespective of their dimensionality.

Oligopyridines[9] are among the most popular and versatile of ligands. The simplest, bipyridine, possesses six isomers with varying directional properties (Scheme 1). 2,2′-Bipyridine (2,2′-bpy or bpy) is tailor-made to act as a chelating ligand, whereas the 4,4′-isomer is commonly used as a rigid, bridging linker in multinuclear complexes and coordination polymers. In contrast, the coordinating abilities of 2,3′-, 2,4′-, 3,3′- and 3,4′-bpy are less well investigated.[1] Terpyridine possesses 48 isomers, of which the bis-chelating 2,2′:6′,2′′-terpyridine (tpy) is the best known. Synthetic routes to terpyridines allow tpy to be readily functionalized in the 4′-position. With the correct choice of substituent X, octahedral {M(4′-Xtpy)$_2$} complexes (Scheme 2) are ideal building blocks for the assembly of
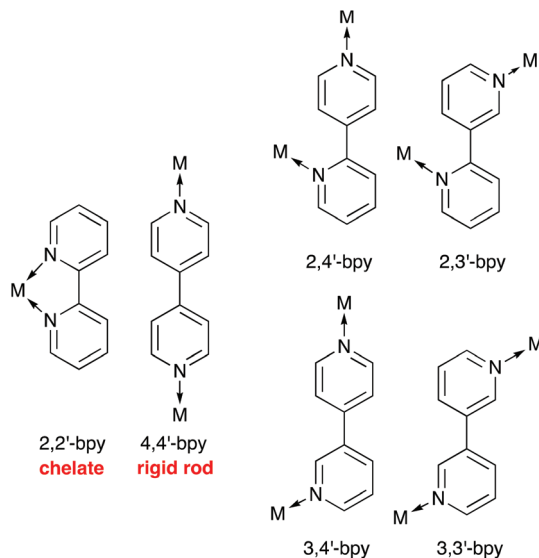
Scheme 1 Isomer dependence of the directional metal-binding properties of bipyridine.
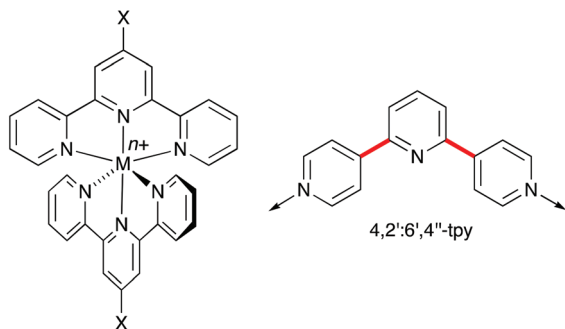
Scheme 2 The $\{M(4'-Xtpy)_2\}^{n+}$ 'expanded ligand' (4′-Xtpy = a general 4′-substituted 2,2′:6′,2″-terpyridine) where X contains a donor group, and the structure of 4,2′:6′,4″-terpyridine. Rotation about the red C–C bonds does not affect the directional properties of the N,N′-donor set.

coordination polymers.[10,11] Whereas tpy is typically a 'convergent' ligand (*i.e.* the chelate effect favours a *cis,cis*-conformation when tpy binds a metal ion), 4,2′:6′,4″-tpy presents a divergent set of donor atoms. Rotation about the inter-ring bonds (in red in Scheme 2) has no effect of the vectorial properties of the N,N′-donor set of 4,2′:6′,4″-tpy. The ligand typically binds metal ions through the outer two N-donors, leaving the central donor uncoordinated. It is, therefore, highly suitable as a building block for coordination polymers.

This article focuses on systematic approaches to the assembly of coordination polymers built upon 4,2′:6′,4″-tpy, and the structural diversity achieved through (i) functionalizing the ligand and (ii) varying the metal-containing domains (nodes). Underlying much of the discussion is the tenet that coordination polymer assembly is a matter of complementarity between the coordination requirements (geometry) of a metal centre and the spatial properties, coordinating ability and packing potential of the linking ligand. The first report of a

coordination polymer involving 4,2′:6′,4″-tpy appeared in 1998,[12] and a search of the Cambridge Structural Database[13] (CSD version 5.35) using Conquest v. 1.15[14] reveals 62 coordination polymers and networks in which 4,2′:6′,4″-tpy or 4′-X-4,2′:6′,4″-tpy (X = various substituents) ligands bridge between two (or three if X is a donor such as a pyridyl substituent) metal centres. This is not a comprehensive account of these 62 structures, rather, in keeping with the spirit of a *Dalton Transactions* perspective review, it is a discussion of significant aspects arising from observations of the assembly processes using these divergent ligands.

The metal-based node

The d-block contains 30 metals with oxidation states and associated electronic configurations that dictate chemistry and coordination geometry of the metal ions. Our own studies of the assembly of coordination polymers tend to favour the use of d^5 or d^{10} metal ions which are electronically spherically symmetric. The geometrical flexibility of d^5 or d^{10} metal centres allows the coordination sphere to respond to environmental influences such as crystal packing interactions. For example, the angles within a 'tetrahedral' zinc(II) centre may lie well outside an ideal 109.5°. In a coordination polymer, distortions within the local coordination environment of the metal ion are transmitted through bridging ligands, and in the next section, we explore how this manifests itself in the pitch of a helical assembly.

In addition to its geometrical flexibility, zinc(II) has a propensity to associate with carboxylate anions to form $\{Zn_2(\mu\text{-}O_2CR)_4\}$ motifs with 'paddle-wheel' structures (Scheme 3). These and related building blocks are popular choices as nodes in coordination polymers and MOFs because they impart directional control on the assembly process.[15–17] In this review, we consider examples of the *in situ* assembly of discrete $\{Zn_2(\mu\text{-}OAc)_4\}$ units, and association with bridging ligands into vacant coordination sites (Scheme 3) to give one-dimensional polymers. This contrasts with the use of organic linkers bearing, typically, two terminal carboxylate groups which become an integral part of the paddle-wheel to generate three-dimensional MOFs.[15,17] As Scheme 3 illustrates, a $\{Zn_2(\mu\text{-}O_2CR)_4\}$ unit necessarily binds axial ligands that are disposed linearly with respect to one another. The consequences of choosing zinc(II) acetate *versus* zinc(II) halides for combination with 4,2′:6′,4″-tpy ligands will become apparent in the
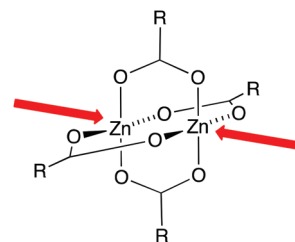
Scheme 3 $\{Zn_2(\mu\text{-}O_2CR)_4\}$ paddle-wheel building block; red arrows mark vacant coordination sites.

Table 1 Comparison of $[ZnCl_2(4'\text{-}X\text{-}4,2':6',4''\text{-}tpy)]_n$ helical coordination polymers

Coordination polymer[a]	Space group	Number of $\{ZnY_2(tpy)\}$ units per turn	Angle N–Zn–N/°	Pitch of helix[b] (Zn⋯Zn/Å)	CSD refcode	Ref.
Heterochiral polymers						
$rac\text{-}[ZnCl_2(4,2':6',4''\text{-}tpy)]_n$	$P2_1/n$	2	98.6(2)	14.078(2)	GAQYUS	12
$rac\text{-}[ZnCl_2(4'\text{-}(4\text{-}MeC_6H_4)\text{-}4,2':6',4''\text{-}tpy)]_n$	$P2_1/n$	2	99.5(1)	16.950(2)	LOCTED	19
$rac\text{-}[ZnCl_2(4'\text{-}(4\text{-}EtC_6H_4)\text{-}4,2':6',4''\text{-}tpy)]_n$	$P2_1/n$	2	93.5(1)	7.790(2)	NOGFOF	19
$rac\text{-}[ZnCl_2(4'\text{-}(4\text{-}pyridyl)\text{-}4,2':6',4''\text{-}tpy)]_n$	$P2_1/n$	2	108.3(1)	20.661(3)	AGUPEY	23
$rac\text{-}[ZnCl_2(4'\text{-}(4\text{-}{}^nC_8H_{17}OC_6H_4)\text{-}4,2':6',4''\text{-}tpy)]_n$	$P2_1/c$	2	104.0(1)	19.3139(7)	AJURIG	20
$rac\text{-}[Zn(OAc)_2(4'\text{-}Ph\text{-}4,2':6',4''\text{-}tpy)]_n$	$P2_1/n$	2	106.99(5)	19.653(4)	CUXDOP	24
$rac\text{-}[Zn(OAc)_2(4'\text{-}(4\text{-}anthracen\text{-}9\text{-}yl\text{-}C_6H_4)\text{-}4,2':6',4''\text{-}tpy)]_n$	$Pnna$	2	114.29(8)	20.893(3)	[c]	25
$rac\text{-}[ZnCl_2(4'\text{-}Ph\text{-}4,2':6',4''\text{-}tpy)]_n$	$P2_1/n$	2	105.9(1)	19.301(2)	FEPRUO	18
$rac\text{-}[ZnI_2(4'\text{-}{}^tBu\text{-}4,2':6',4''\text{-}tpy)]_n$	$P2_1/c$	2	105.0(1)	18.158(1)	FAKRUG	26
Homochiral polymers						
$M\text{-}[ZnCl_2(4'\text{-}(4\text{-}MeC_6H_4)\text{-}4,2':6',4''\text{-}tpy)]_n$	$P3_121$	3	100.3(2), 107.9	32.414(5)	NOGFIZ	19
$M\text{-}[Zn(OAc)_2(4'\text{-}(4\text{-}anthracen\text{-}9\text{-}yl\text{-}C_6H_4)\text{-}4,2':6',4''\text{-}tpy)]_n$	$P2_12_12_1$	2	104.5(3)	17.979(1)	[c]	25

[a] Solvent molecules are omitted from formulae of NOGFOF, FAKRUG and the 4'-(4-anthracen-9-yl-C₆H₄) derivatives. [b] Pitch is measured from one Zn atom to the next which is the point the helix maps back onto itself. [c] Compound not yet entered in CSD v. 5.35.

following discussion. We will also comment on the effects of moving from first to third row d[10] metals which introduces larger metal ions that can accommodate higher coordination numbers.

All things helical

Our initial foray into the metal-binding abilities of 4'-functionalized 4,2':6',4''-tpy ligands was against a backdrop of a few one-dimensional polymers of the type $[ZnCl_2(4'\text{-}X\text{-}4,2':6',4''\text{-}tpy)]_n$ in which X = H,[12] Ph,[18,19] 4-MeC₆H₄,[19] 4-EtC₆H₄,[19] and 4-${}^nC_8H_{17}OC_6H_4$.[20] All polymers discussed in this section contain achiral building blocks, but when the chain is built upon a crystallographic screw axis, it is helical and, therefore, chiral. Related to the complexes discussed below are $[ZnY_2\text{-}(4'\text{-}(4\text{-}(3\text{-}chloropyridyl))\text{-}4,2':6',4''\text{-}tpy)]_n$ (Y = Cl or I)[21] and $[ZnI_2(4'\text{-}(4\text{-}pyridyl)\text{-}4,2':6',4''\text{-}tpy)]_n$.[22] In each, the chain is built up by a glide plane rather than a screw axis, and hence a helical description is not appropriate.

Table 1 summarizes the current status of one-dimensional $[ZnCl_2(4'\text{-}X\text{-}4,2':6',4''\text{-}tpy)]_n$ helical coordination polymers. Note that most structures are free of solvent of crystallization (see footnote to Table 1). Typically, crystallization results in an equal number of right-handed (P) and left-handed (M) helices in the same lattice, *i.e.* a *rac-* or heterochiral polymer, which is to be distinguished from a racemic conglomerate (a mixture of crystals, each of which contains one enantiomer). Table 1 lists two homochiral polymers, and for both, the corresponding heterochiral polymers have also isolated.[19,25] The distance between the outer N-donors in 4,2':6',4''-tpy is independent of whether the ligand is planar or twisted about the C–C bonds marked in red in Scheme 2, and so the distance between adjacent Zn²⁺ ions along a chain shows little variation (12.379(2) to 13.207(2) Å). However, the pitch of the helix is noticeably variable. $M\text{-}[ZnCl_2(4'\text{-}(4\text{-}MeC_6H_4)\text{-}4,2':6',4''\text{-}tpy)]_n$ is unique among the polymers in Table 1; it crystallizes in the $P3_121$ space group with the helical chain generated by a 3_1-screw axis. Each
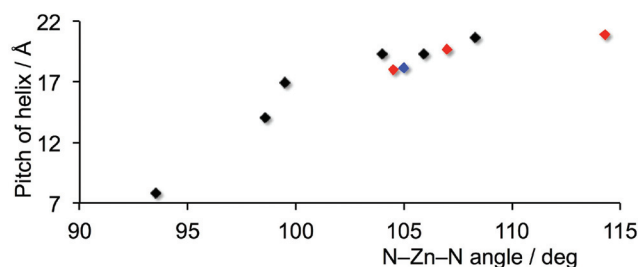

Fig. 1 Scatter plot of N–Zn–N angle against helical pitch of the one-dimensional coordination polymers in Table 1 which contain two $\{ZnY_2(tpy)\}$ units per helical-turn; Y = Cl, black; Y = I, blue; Y = monodentate OAc, red.

turn in the helix contains three $\{ZnY_2(tpy)\}$ units and the helical pitch of 32.414(5) Å is significantly longer than those of the remaining polymers, each of which contains two $\{ZnY_2(tpy)\}$ units per helical-turn. For the latter, the data in Table 1 and Fig. 1 confirm a general relationship between the helical pitch and the N–Zn–N bond angle, and we consider below how this variation is associated with crystal packing.

Of the polymers in Table 1, $rac\text{-}[ZnCl_2(4'\text{-}(4\text{-}EtC_6H_4)\text{-}4,2':6',4''\text{-}tpy)]_n$ stands out as possessing a very short helical pitch (7.790(2) Å).[19] This follows from the interdigitation of adjacent chains of the same handedness. Fig. 2a views part of the lattice down the *b*-axis, parallel to which the helical chains run. Helices of a given chirality are interlocked, generating infinite pillars of π-stacked phenylpyridine domains of adjacent P- (or M-) chains (Fig. 2a and 2b). The lattice consists of alternating homochiral layers of P- or M-helical polymers, each layer lying parallel to the *ab*-plane. The factors that underlie homochiral *versus* heterochiral packing fascinate and challenge researchers,[27] and it is noteworthy that the racemic polymers in the $[ZnY_2(4'\text{-}X\text{-}4,2':6',4''\text{-}tpy)]_n$ family (Table 1) include both those with homochiral layers (noted by Li and coworkers in 2008 as 'very rare'[19]) and those in which P- and M-helices
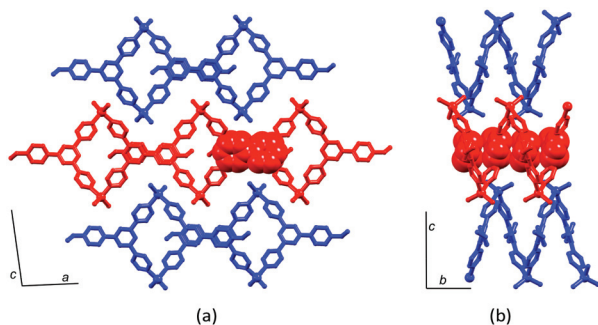
Fig. 2 Packing of *P*- and *M*-chains of [ZnCl$_2$(4′-(4-EtC$_6$H$_4$)-4,2′:6′,4′′-tpy)]$_n$. Helical chains follow the *b*-axis. (a) View down the *b*-axis showing rows of interdigitated helices of the same handedness; (b) view down the *a*-axis emphasizing the shallow pitch of each helix. Chains of opposite handedness are coloured red and blue.
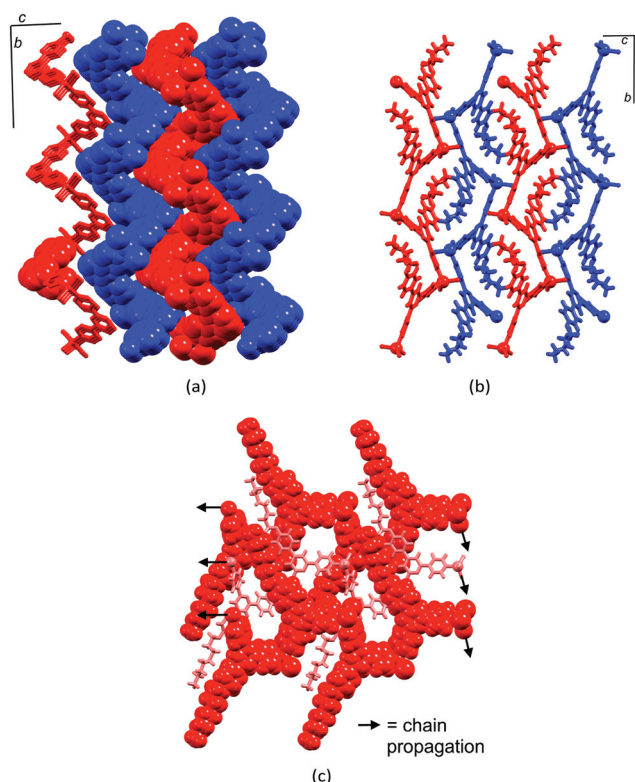

Fig. 3 Packing of *P*- and *M*-chains into homochiral layers in (a) *rac*-[ZnCl$_2$(4,2′:6′,4′′-tpy)]$_n$ and (b) *rac*-[ZnCl$_2$(4′-(4-^{n}C$_8$H$_{17}$OC$_6$H$_4$)-4,2′:6′,4′′-tpy)]$_n$. Each chain runs parallel to the *b*-axis, and layers lie parallel to the *ab*-plane. Chains of opposite handedness are coloured red and blue. In (a), a representative π-stacking interaction between chains of the same handedness is shown in the layer on the left-side of the figure. (c) Part of one homochiral sheet in *rac*-[ZnCl$_2$(4′-(4-^{n}C$_8$H$_{17}$OC$_6$H$_4$)-4,2′:6′,4′′-tpy)]$_n$, showing alignment of the alkyl chains.

Fig. 4 Packing of *P*- and *M*-chains in (a) *rac*-[ZnCl$_2$(4′-(4-MeC$_6$H$_4$)-4,2′:6′,4′′-tpy)]$_n$, and (b) *rac*-[ZnCl$_2$(4′-(4-pyridyl)-4,2′:6′,4′′-tpy)]$_n$. Chains of opposite handedness are coloured red and blue, and representative π-stacking interactions are shown in space-filling representation.

assembly is observed in *rac*-[ZnCl$_2$(4′-(4-^{n}C$_8$H$_{17}$OC$_6$H$_4$)-4,2′:6′,4′′- tpy)]$_n$ (Fig. 3b).[20] In this case, the 4′-substituent is a long alkyl chain and CH$_{alkyl\ chain}$···π$_{phenyl}$ and CH$_{alkyl\ chain}$···π$_{pyridine}$ are dominant packing interactions within each homochiral sheet; the packing of polymer chains of the same handedness is illustrated in Fig. 3c.

The presence of homochiral sheets in the lattice is predicated upon a recognition event occurring between a helical chain of a given chirality with an adjacent chain of the same chirality. This occurs in three of the nine racemates in Table 1. In the remaining six, packing interactions occur only between *P*- and *M*-helices. Adjacent *P*- and *M*-chains in *rac*-[ZnCl$_2$(4′-(4-MeC$_6$H$_4$)-4,2′:6′,4′′-tpy)]$_n$ engage in face-to-face π-interactions between pyridine rings (Fig. 4a); Li and coworkers comment that 'the whole crystal presents a heterochiral packing'.[19] Analogous behaviour is observed in *rac*-[ZnCl$_2$(4′-(4-pyridyl)-4,2′:6′,4′′-tpy)]$_n$ (Fig. 4b).[23] In *rac*-[ZnCl$_2$(4′-Ph-4,2′:6′,4′′-tpy)]$_n$[18] and *rac*-[Zn(OAc)$_2$(4′-Ph-4,2′:6′,4′′-tpy)]$_n$,[24] *P*- and *M*-chains associate through π-stacking of tpy domains in adjacent helices. The change from chlorido to acetato ligands in the latter two polymers perturbs the structure only slightly. Note that each of the above four compounds has a similar 4′-aromatic substituent (phenyl, tolyl or pyridyl) and the polymers pack in similar, heterochiral fashions; each crystallizes with no solvent in the lattice. In *rac*-[ZnI$_2$(4′-^{t}Bu-4,2′:6′,4′′-tpy)·1,2-Cl$_2$C$_6$H$_4$]$_n$, π-stacking between pyridine rings of tpy domains in adjacent *P*- and *M*-helices occurs (Fig. 5), interconnecting the chains throughout the lattice. The aromatic solvent molecules are intimately involved in π-stacking in the lattice, extending each double stack in Fig. 5 to a quadruple-decker arrangement.[26]

We have recently been examining the effects of introducing extended arene domains in the 4′-position of 4,2′:6′,4′′-tpy, with the supposition that enhancement of arene···arene π-stacking interactions should provide some degree of control over crystallization events. The isolation of crystals of both

are always adjacent to one another. However, there appears to be no obvious trend that links the 4′-substituent to the mode of packing. In *rac*-[ZnCl$_2$(4,2′:6′,4′′-tpy)]$_n$ (no 4′-substituent),[12] *P*- (or *M*-) helices associate through π-stacking between pyridine rings in adjacent chains of the same handedness forming homochiral two-dimensional sheets (Fig. 3a). A similar
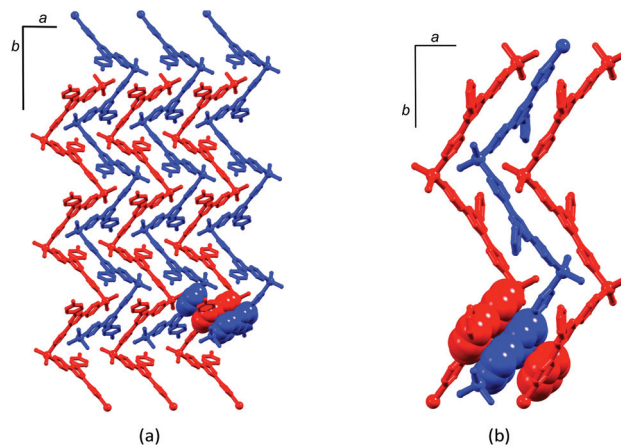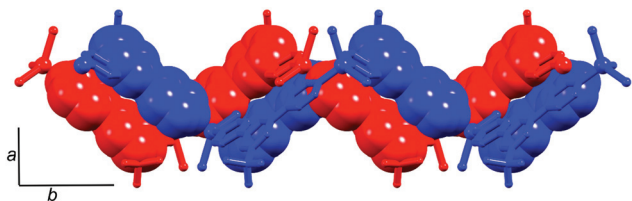
Fig. 5 Interlocking of *P*- and *M*-helices in *rac*-[ZnI₂(4′-ᵗBu-4,2′:6′,4″-tpy)]ₙ; face-to-face interactions of tpy domains are shown in space-filling representations.

(a)

(b)
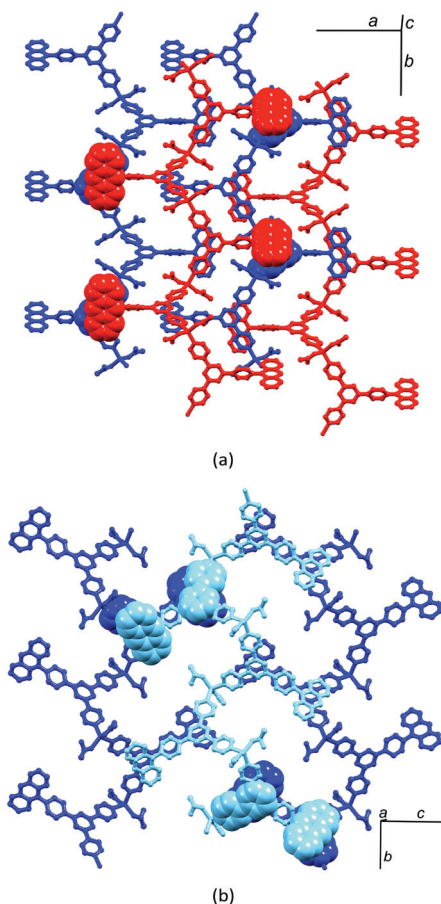
Fig. 6 (a) Packing of two *P*- (blue) and two *M*- (red) helical chains in *rac*-[Zn(OAc)₂(4′-(4-anthracen-9-yl-C₆H₄)-4,2′:6′,4″-tpy)]ₙ. (b) Anthracene···tpy stacking interactions between adjacent chains in *M*-[Zn(OAc)₂(4′-(4-anthracen-9-yl-C₆H₄)-4,2′:6′,4″-tpy)]ₙ. Representative anthracene···tpy interactions are in space-filling depiction.

homo- and heterochiral [Zn(OAc)₂(4′-(4-anthracen-9-yl-C₆H₄)-4,2′:6′,4″-tpy)]ₙ from the same crystallization tube[25] illustrates how unpredictable the crystallization process can be. Serendipity is ever present, and we are a long way from being to drive these systems in a particular direction. The helical pitch in *rac*-[Zn(OAc)₂(4′-(4-anthracen-9-yl-C₆H₄)-4,2′:6′,4″-tpy)]ₙ is ≈3 Å longer than in the enantiomerically pure *M*-helix (Table 1). Fig. 6 illustrates the packing of chains in the hetero- and homochiral structures. In both, face-to-face π-stacking between tpy and anthracene domains is dominant, but a comparison of

Fig. 6a and 6b reveals the distinct ways in which chains of opposite handedness and of the same handedness associate with one another in heterochiral and homochiral coordination polymers, respectively.

Closing the loop

In the previous section, we saw that a combination of zinc(ɪɪ) halides and 4′-X-4,2′:6′,4″-tpy ligands in which the 4′-substituent X is, in general, coordinatively innocent yields a one-dimensional polymer. However, we have recently found that under room temperature crystallization conditions using layering of solutions of ZnCl₂ or ZnBr₂ and a 4′-X-4,2′:6′,4″-tpy ligand, it is also possible to isolate the discrete metallohexacyclic complexes [{ZnY₂(4′-X-4,2′:6′,4″-tpy)}₆] (Y = Cl or Br). First observed for [{ZnCl₂(4′-HC≡CC₆H₄-4,2′:6′,4″-tpy)}₆]²¹ (Fig. 7a), we have since noted that metallomacrocycles are especially prevalent when extended arene domains are present in the ligand (Scheme 4). It is likely that this is associated with the manner in which the metallohexacycles nest inside one another (see below). Lattices of [{ZnY₂(4′-X-4,2′:6′,4″-tpy)}₆] metallomacrocycles contain large void spaces and crystallize as solvates; crystals are very sensitive to solvent loss, making their manipulation and structure determination challenging.²⁸
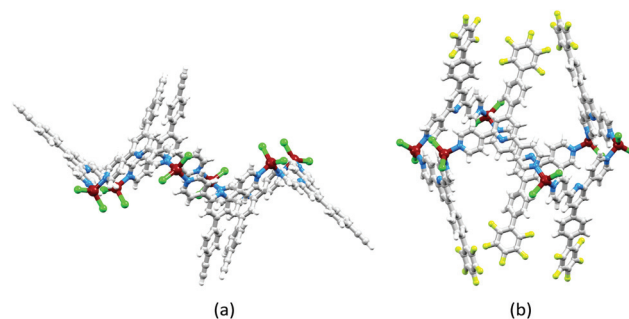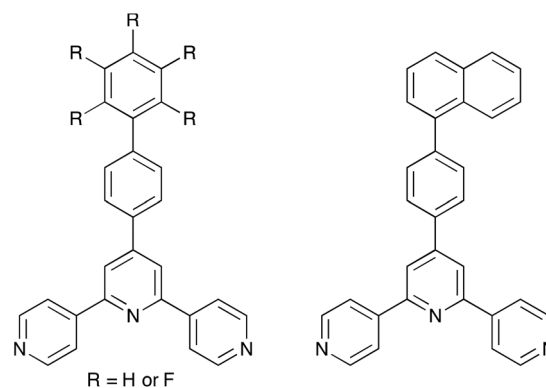

(a)

(b)

Fig. 7 (a) Chair-like conformation of [{ZnCl₂(4′-HC≡CC₆H₄-4,2′:6′,4″-tpy)}₆], also adopted by [{ZnCl₂(4′-(4-C₆F₅)C₆H₄-4,2′:6′,4″-tpy)}₆] (b) Barrel-like conformer of [{ZnCl₂(4′-(4-C₆F₅)C₆H₄-4,2′:6′,4″-tpy)}₆].

Scheme 4 Examples of 4′-X-4,2′:6′,4″-tpy ligands with extended arene functionalities.

In [{ZnCl$_2$(4'-HC≡CC$_6$H$_4$-4,2':6',4''-tpy)}$_6$], each 4,2':6',4''-tpy unit bridges two ZnCl$_2$ units, and each Zn^{2+} ion is tetrahedrally sited. The conformation of the ring may be described as chair-like, but it is useful to note that this corresponds to an up/up/up/down/down/down arrangement of ligands (Fig. 7a).[21] This same arrangement is found for [{ZnCl$_2$(4'-(pentafluoro-biphenyl-4-yl)-4,2':6',4''-tpy)}$_6$] but, in this case, this is one of two observed conformations; in the second (the minor form), the ligands are in an alternating up/down/up/down/up/down arrangement around the ring (a 'barrel-like' conformation, Fig. 7b). Both conformations were observed in the same crystallization experiment, suggesting little energy difference between them. The barrel conformation is also adopted by [{ZnCl$_2$(4'-(biphenyl-4-yl)-4,2':6',4''-tpy)}$_6$], [{ZnBr$_2$(4'-(biphenyl-4-yl)-4,2':6',4''-tpy)}$_6$], [{ZnBr$_2$(4'-(pentafluorobiphenyl-4-yl)-4,2':6',4''-tpy)}$_6$] and [{ZnBr$_2$(4'-(naphthalen-1-yl)phenyl-4,2':6',4''-tpy)}$_6$], each crystallizing in the trigonal space group $R\bar{3}$.[28] The extended arene domains are the key to extremely efficient packing of the barrels into tubes. The interlocking of metallohexacycles through π-interactions between pyridine and arene domains produces a robust architecture (Fig. 8) and face-to-face π-interactions between tpy units in adjacent tubes further stabilize the lattice.

The organization of the pendant arene moieties (phenyl, pentafluorophenyl or naphthyl groups) and the inner diameter of the tubes suggested to us that the assembly should be amenable to capturing guests such as fullerenes. Indeed, crystallization of 4'-(naphthalen-1-yl)phenyl-4,2':6',4''-tpy with ZnCl$_2$ in the presence of C$_{60}$ led to the host–guest complex shown in Fig. 9. Each C$_{60}$ guest is embraced by six naphthyl units (green in Fig. 9), and the whole domain lies at the centre of
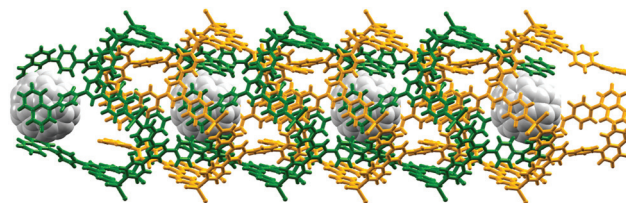

Fig. 9 In [2{ZnCl$_2$(4'-(naphthalen-1-yl)phenyl-4,2':6',4''-tpy)}$_6$·C$_{60}$·6MeOH·16H$_2$O, guest molecules of C$_{60}$ occupy every other cavity in the metallohexacyclic host.

another hexamer (orange in Fig. 9). Highly efficient arene···arene π-interactions operate between layers of the onion-like construction. Two features are particularly remarkable about the structure: (i) the fullerene molecule is crystallographically ordered, and (ii) the lattice is an ordered array in which a C$_{60}$ molecule occupies every second cavity, despite there being room on steric grounds for complete occupation of cavities. We have suggested that the latter observation is closely linked to the manner in which the overall structure is assembled.[28]

The rigidity of the tubes formed by interlocking of [{ZnY$_2$(4'-arene-4,2':6',4''-tpy)}$_6$] metallohexacycles suggests that this family of complexes offers a rich opportunity for further explorations of host–guest chemistry.

Paddle-wheel nodes

Although Table 1 shows examples of one-dimensional coordination polymers containing mononuclear Zn(OAc)$_2$-containing nodes, it is very common for zinc(ɪɪ) carboxylates to form dinuclear, 'paddle-wheel' {Zn$_2$(μ-OAc)$_4$} building blocks.[16,17] An analogous scenario is observed for copper(ɪɪ) acetates. Donors which bind to the axial sites of the {Zn$_2$(μ-O$_2$CR)$_4$} unit (Scheme 3) bear a linear relationship to each other. As a consequence, the directional properties of a one-dimensional coordination polymer containing {Zn$_2$(μ-O$_2$CR)$_4$} nodes are determined by the bridging ligand. Because the N-donors of the outer rings in 4,2':6',4''-tpy subtend an angle of 120°, a [Zn$_2$(μ-O$_2$CR)$_4$(4'-X-4,2':6',4''-tpy)]$_n$ polymer possesses a zigzag backbone (Scheme 5a). Pioneering work from the Newkome group shows how the use of a 1,3-substitution pattern in an arene linker ■ in the ditopic (2,2':6',2''-tpy)-■-(2,2':6',2''-tpy) ligand directs the assembly of a metallohexagon through interconnection of {M(2,2':6',2''-tpy)$_2$} domains.[29] In a similar manner, one can envisage a combination of linear {Zn$_2$(μ-O$_2$CR)$_4$} nodes with divergent 4'-X-4,2':6',4''-tpy linkers being predisposed towards the formation of a metallohexacycle (Scheme 5b). However, to date, this conjecture has not been fulfilled. Instead, one-dimensional polymers persist.

In contrast to the structural variation of the helical polymers in Table 1, [M$_2$(μ-OAc)$_4$(4'-X-4,2':6',4''-tpy)]$_n$ coordination polymers known to date are structurally related, both in the zigzag backbone of the polymer chain and in the packing of the chains in the crystal lattice. Space groups and cell dimensions are compared in Table 2. With the exception of
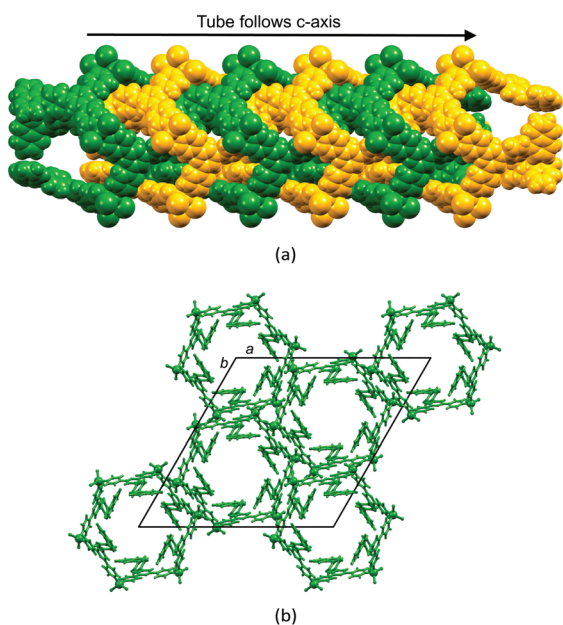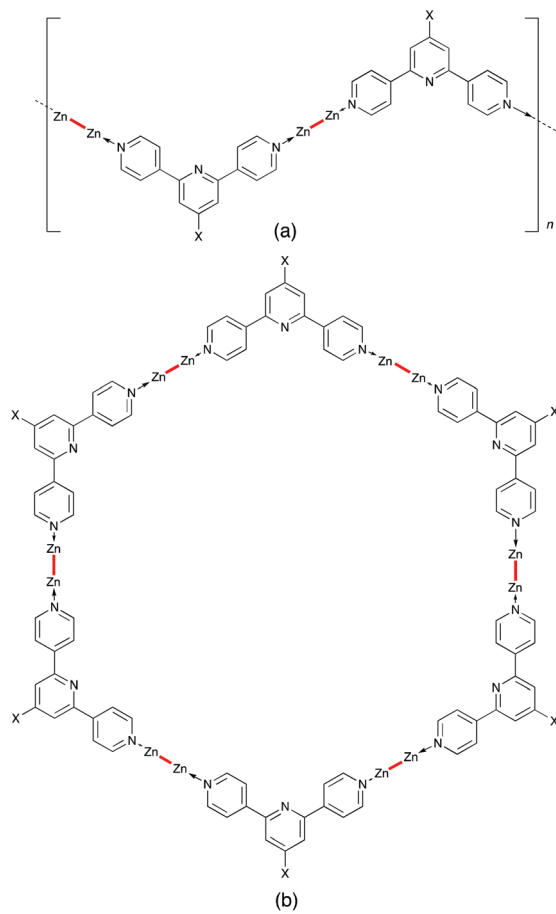

Tube follows c-axis

(a)

(b)

Fig. 8 Packing in the barrel-like conformer of [{ZnBr$_2$(4'-(naphthalen-1-yl)phenyl-4,2':6',4''-tpy)}$_6$] to illustrate: (a) interlocking of hexacycles (all crystallographically equivalent) to form tubes, and (b) alignment of tubes parallel to the c-axis.

Scheme 5 (a) Schematic representation of a [Zn$_2$(μ-O$_2$CR)$_4$(4′-X-4,2′:6′,4″-tpy)]$_n$ polymer (Zn–Zn = Zn$_2$(μ-O$_2$CR)$_4$ unit); (b) proposed metallohexacycle (see text).

[Zn$_2$(μ-OAc)$_4$(4′-(4-MeSC$_6$H$_4$)-4,2′:6′,4″-tpy)]$_n$,[30] all crystallize in the C2/c space group with one half of the 4,2′:6′,4″-tpy ligand in the asymmetric unit and the second half generated by a C$_2$ axis. As a consequence, the ^{t}butyl group in [Zn$_2$(μ-OAc)$_4$-(4′-^{t}Bu-4,2′:6′,4″-tpy)]$_n$, is necessarily disordered.[26] In [Zn$_2$(μ-OAc)$_4$(4′-(4-MeSC$_6$H$_4$)-4,2′:6′,4″-tpy)]$_n$ (P2$_1$/c), the presence of an ordered MeS group is incompatible with a C$_2$ axis through the 4′-(4-MeSC$_6$H$_4$)-4,2′:6′,4″-tpy ligand. Taking this distinction into account, Table 2 shows that the unit cell dimensions of all coordination polymers are comparable.

The structural relationship between the coordination polymers stems from the dominant face-to-face π-interactions between 4,2′:6′,4″-tpy domains of adjacent chains. Fig. 10 illustrates this for [Zn$_2$(μ-OAc)$_4$(4′-(4-BrC$_6$H$_4$)-4,2′:6′,4″-tpy)]$_n$.[30] Zigzag chains nest with one another to generate planar sheets (Fig. 10b) in which each 4-bromophenyl group in one chain is accommodated in the V-shaped cavity formed by a 4,2′:6′,4″-tpy unit in the adjacent chain (Fig. 10a). As the space-filling representation in Fig. 10a suggests, this cavity is big enough to accommodate larger substituents. For example, biphenyl units can be accommodated without significant moving apart of the zigzag chains. This statement is quantified by measuring the

distance d defined in Fig. 10c; values are listed in Table 2 and show only a relatively small variation.

The presence of biphenyl domains in [Zn$_2$(μ-OAc)$_4$-(4′-(biphenyl-4-yl)-4,2′:6′,4″-tpy)]$_n$ and [Cu$_2$(μ-OAc)$_4$(4′-(biphenyl-4-yl)-4,2′:6′,4″-tpy)]$_n$ leads to inter-chain biphenyl···biphenyl stacking[31] which augments the tpy···tpy interactions between sheets. Interestingly, introducing fluoro-substituents into the terminal phenyl ring of the biphenyl unit has little impact on the packing of the chains. Thus, on going from [Cu$_2$(μ-OAc)$_4$(4′-(biphenyl-4-yl)-4,2′:6′,4″-tpy)]$_n$ to [Cu$_2$(μ-OAc)$_4$-(4′-(pentafluorobiphenyl-4-yl)-4,2′:6′,4″-tpy)]$_n$, tpy···tpy stacking interactions are maintained, arene···arene π$_H$···π$_H$ interactions are replaced by π$_H$···π$_F$, and H···H contacts are replaced by H···F interactions.[32]

The complex [Zn$_2$(μ-OAc)$_4$(4′-Ph-4,2′:6′,4″-tpy)]$_n$ is unique among the series in Table 2 because it crystallizes as a solvate, viz. [Zn$_2$(μ-OAc)$_4$(4′-Ph-4,2′:6′,4″-tpy)]$_n$·0.3CH$_2$Cl$_2$. It is noteworthy that the partial occupancy CH$_2$Cl$_2$ molecules are located in sites that coincide with those occupied by the para-substituents of the phenyl rings in [Zn$_2$(μ-OAc)$_4$(4′-(4-ZC$_6$H$_4$)-4,2′:6′,4″-tpy)]$_n$ (Z = Br, MeS or Ph).[32] Undoubtedly, there has to be a limiting point at which the structure can no longer withstand the steric demands of this substituent. Indeed, we have reported that the reaction of zinc(II) acetate with 4′-(4-dodecyl-oxyphenyl)-4,2′:6′,4″-tpy leads, not to a polymer, but to the discrete molecule [Zn$_2$(μ-OAc)$_4$(4′-(4-dodecyloxyphenyl)-4,2′:6′,4″-tpy)$_2$].[33] We are currently undertaking a systematic study to better understand how the structure type shown in Fig. 10 responds to increasingly larger substituents appended to the 4′-position of 4,2′:6′,4″-tpy.

A tendency to cluster

We have seen how the tendency for zinc(II) and copper(II) acetate to form paddle-wheel motifs dictates the linear relationship of the coordinated N-donors. Although these motifs are extremely common,[17] higher nuclearity clusters are also well established.[15] However, rationalizing, let alone predicting, their formation is problematic, if not impossible, as examples from our recent work illustrate. While reactions of Zn(OAc)$_2$·2H$_2$O with 4′-(biphenyl-4-yl)-4,2′:6′,4″-tpy or Cu(OAc)$_2$·H$_2$O with 4′-(biphenyl-4-yl)-4,2′:6′,4″-tpy and/or 4′-(pentafluoro-biphenyl-4-yl)-4,2′:6′,4″-tpy (Scheme 4) yield one-dimensional polymers supported by the anticipated paddle-wheel {M$_2$(μ-OAc)$_4$} nodes (Table 2), the reaction of Zn(OAc)$_2$·2H$_2$O with 4′-(pentafluorobiphenyl-4-yl)-4,2′:6′,4″-tpy results in crystals of [Zn$_2$(μ-OAc)$_4$(4′-(pentafluorobiphenyl-4-yl)-4,2′:6′,4″-tpy)]$_n$ and [{Zn$_5$(OAc)$_{10}$(4′-(pentafluorobiphenyl-4-yl)-4,2′:6′,4″-tpy)}·11H$_2$O]$_n$ in the same crystallization tube.[32] X-Ray powder diffraction data for the bulk sample reveal that the polymer containing pentanuclear {Zn$_5$(OAc)$_{10}$} nodes is the dominant product. This polymer (Fig. 11) is significant for a number of reasons: (i) the 5 : 4 ratio of zinc atoms : tpy ligands which leads to a highly unusual network (Fig. 11a), (ii) the structure of the {Zn$_5$(OAc)$_{10}$} unit which, to the best of our knowledge, is unprecedented, and (iii) the assembly of a quadruple-stranded chain (Fig. 11b) that is a 'deep' version of the single-stranded

Table 2 Comparison of $[M_2(\mu\text{-OAc})_4(4'\text{-X-4},2'\text{:}6',4''\text{-tpy})]_n$ (M = Zn or Cu) one-dimensional coordination polymers

Coordination polymer[a]	Space group	a, b, c/Å	β/°	Distance d/Å (defined in Fig. 10c)	CSD refcode	Ref.
$[Zn_2(\mu\text{-OAc})_4(4'\text{-Ph-4},2'\text{:}6',4''\text{-tpy})]_n$	$C2/c$	26.1802(6) 15.2942(6) 8.0478(2)	107.449(2)	12.495	CUXDUV	24
$[Zn_2(\mu\text{-OAc})_4(4'\text{-}(4\text{-BrC}_6\text{H}_4)\text{-4},2'\text{:}6',4''\text{-tpy})]_n$	$C2/c$	26.0368(8) 15.0774(5) 8.0056(3)	107.238(2)	12.268	CUXCOO	30
$[Zn_2(\mu\text{-OAc})_4(4'\text{-}(4\text{-MeSC}_6\text{H}_4)\text{-4},2'\text{:}6',4''\text{-tpy})]_n$	$P2_1/c$	8.1338(4) 14.9020(7) 25.2700(10)	90.457(3)	12.092	CUXCUU	30
$[Zn_2(\mu\text{-OAc})_4(4'\text{-(biphenyl-4-yl)-4},2'\text{:}6',4''\text{-tpy})]_n$	$C2/c$	26.210(5) 16.151(2) 8.3410(5)	108.050(14)	13.347	RIJFUN	31
$[Cu_2(\mu\text{-OAc})_4(4'\text{-(biphenyl-4-yl)-4},2'\text{:}6',4''\text{-tpy})]_n$	$C2/c$	26.0528(9) 16.1512(9) 8.2267(3)	108.113(2)	13.346	RIGJAU	31
$[Cu_2(\mu\text{-OAc})_4(4'\text{-(pentafluorobiphenyl-4-yl)-}4,2'\text{:}6',4''\text{-tpy})]_n$	$C2/c$	26.5522(13) 16.7313(9) 8.0639(4)	107.038(3)	13.942	^{b}	32
$[Cu_2(\mu\text{-OAc})_4(4'\text{-(biphenyl-4-yl)-4},2'\text{:}6',4''\text{-tpy})]_n\cdot[Cu_2(\mu\text{-OAc})_4\text{-}(4'\text{-(pentafluorobiphenyl-4-yl)-}4,2'\text{:}6',4''\text{-tpy})]_n$	$C2/c$	26.366(3) 16.393(2) 8.1433(9)	107.648(6)	13.602	^{b}	32
$[Zn_2(\mu\text{-OAc})_4(4'\text{-}^t\text{Bu-4},2'\text{:}6',4''\text{-tpy})]_n$	$C2/c$	26.316(6) 14.8918(19) 8.0849(17)	105.687(17)	12.088	FAKROA	26

^{a} Solvent molecules are omitted from formulae of CUXDUV. ^{b} Compound not yet entered in CSD v. 5.35.

chains exhibited by $\{Zn_2(\mu\text{-OAc})_4\}$-containing coordination polymers (Table 2). These 'deep' chains are stabilized by intra-chain face-to-face stacking of pentafluorobiphenyl domains (Fig. 11b) and pack in an analogous manner to the single-stranded chains shown in Fig. 10.

Multiple strands in one-dimensional coordination polymers containing $4,2'\text{:}6',4''$-tpy ligands are not restricted to the example above. Double-stranded chains are observed in $[Cd_2(OAc)_4(4'\text{-(biphenyl-4-yl)-4},2'\text{:}6',4''\text{-tpy})_2]_n$[31] (Fig. 12a). The $\{Cd_2(OAc)_4\}$ node does not mimic the paddle-wheel of its iso-electronic $\{Zn_2(OAc)_4\}$ counterpart, but instead adopts the planar structure shown in Fig. 12b; the larger size of the Cd^{2+} ion permits a higher coordination number with respect to Zn^{2+}. Extension to a trinuclear node is exemplified by the planar $\{Mn_3(OAc)_6\}$ unit containing manganese(II) (Fig. 12c). These nodes are interconnected by $4'\text{-}(4\text{-BrC}_6\text{H}_4)\text{-4},2'\text{:}6',4''$-tpy bridging ligands in $[Mn_3(OAc)_6(4'\text{-}(4\text{-BrC}_6\text{H}_4)\text{-4},2'\text{:}6',4''\text{-tpy})_3]_n$ to generate a triple-stranded one-dimensional polymer (Fig. 12d). Both multiply-stranded zigzag chains exhibit intra- and inter-chain face-to-face π-stacking of tpy domains, and packing characteristics of the 'deep' chains mimic those of the simpler single-stranded systems.

There are clearly points that relate the structures of the single, double, triple and quadruple-stranded coordination polymers. On the one hand, it is a trivial task to explain how the single strands are propagated from paddle-wheel motifs that are predictably linear nodes (Scheme 3). It is also straight-forward to understand how the planar $\{Cd_2(OAc)_4\}$ and $\{Mn_3(OAc)_6\}$ nodes bind divergent $4,2'\text{:}6',4''$-tpy linkers to produce double and triple-stranded polymers, respectively.

However, it is difficult to rationalize why the $\{Zn_5(OAc)_{10}\}$ motifs bind four ligands to give the oblique arrangement shown in Fig. 11, rather than five to generate a parallel arrangement akin to the double and triple-stranded assemblies.

Although crystallization of $Zn(OAc)_2\cdot2H_2O$ with $4'\text{-(naphtha-len-1-yl)phenyl-4},2'\text{:}6',4''$-tpy (Scheme 4) typically gives $[Zn_2\text{-}(\mu\text{-OAc})_4(4'\text{-(naphthalen-1-yl)phenyl-4},2'\text{:}6',4''\text{-tpy})]_n$, a few crystals of the homochiral polymer $2[\{Zn_7(\mu\text{-OAc})_{10}(\mu_4\text{-O})_2(4'\text{-}(naphthalen-1-yl)phenyl-4},2'\text{:}6',4''\text{-tpy})\}_n]\cdot CH_2Cl_2$ (Fig. 13) have also been isolated.[25] The nodes in this one-dimensional chain are $\{Zn_7(\mu\text{-OAc})_{10}(\mu_4\text{-O})_2\}$ clusters (Fig. 13a), a building block that also appears in several other coordination polymers.[34] The reasons behind this assembly and why chiral resolution is observed remain unknown. However, these findings constitute a word of caution in terms of drawing in-depth conclusions based on single-point structure determinations, and empha-size the need for powder diffraction data for bulk samples.

Conclusions

This perspective review has considered a number of pertinent aspects of the coordination chemistry of the divergent $4,2'\text{:}6',4''$-terpyridine ligand. The ready functionalization of $4,2'\text{:}6',4''$-tpy in the $4'$-position allows one to synthesize a range of ligands in which the $4'$-substituent can be selected to assist in directing the metal–ligand coordination process. Combined with zinc(II) halides, $4'\text{-X-4},2'\text{:}6',4''$-tpy ligands show a tendency to form one-dimensional coordination polymers which are
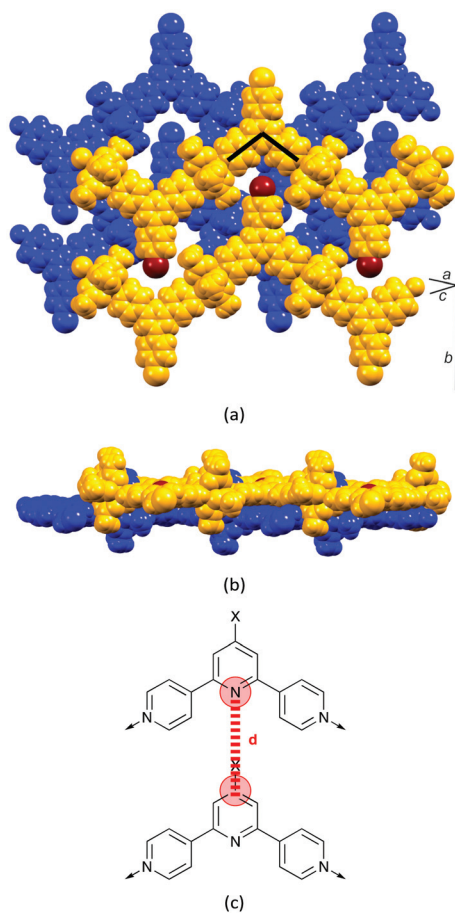
(a)

(b)

(c)

Fig. 10 Packing of zigzag chains in $[Zn_2(\mu\text{-OAc})_4(4'\text{-}(4\text{-BrC}_6H_4)\text{-}4,2':6',4''\text{-tpy})]_n$. (a) Zigzag chains nest with one another to give sheets (blue and orange), and tpy domains (one is represented by a ^) in one sheet stack over tpy domains in the next sheet. See text for discussion of the Br (brown) atoms. (b) The sheets are flat. (c) The distance between central pyridine rings in each sheet (defined as d) varies only slightly with substituent X (see Table 2).
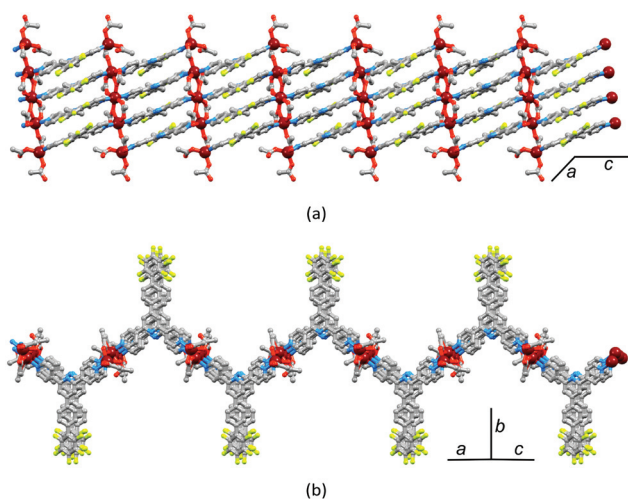

(a)

(b)

Fig. 11 Views of part of one of the quadruple-stranded chains in $[\{Zn_5(OAc)_{10}(4'\text{-}(pentafluorobiphenyl\text{-}4\text{-yl})\text{-}4,2':6',4''\text{-tpy})\}\cdot 11H_2O]_n$. (a) Each chain consists of $\{Zn_5(OAc)_{10}\}$ motifs interconnected by four tpy ligands; (b) view perpendicular to that in (a) showing the face-to-face stacking of pentafluorobiphenyl domains.
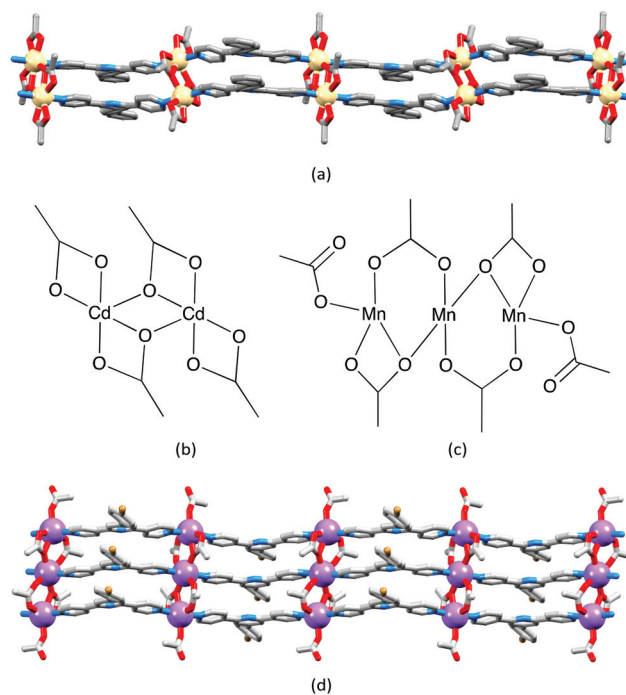
(a)

(b)

(c)

(d)

Fig. 12 (a) Part of one of the double-stranded chains in $[Cd_2(OAc)_4(4'\text{-}(biphenyl\text{-}4\text{-yl})\text{-}4,2':6',4''\text{-tpy})_2]_n]$. (b) and (c) Structures of the planar $\{Cd_2(OAc)_4\}$ and $\{Mn_3(OAc)_6\}$ nodes; N-donors bind above and below the plane. (d) Part of one of the triple-stranded chains in $[Mn_3(OAc)_6(4'\text{-}(biphenyl\text{-}4\text{-yl})\text{-}4,2':6',4''\text{-tpy})_2]_n$.

(a)

(b)

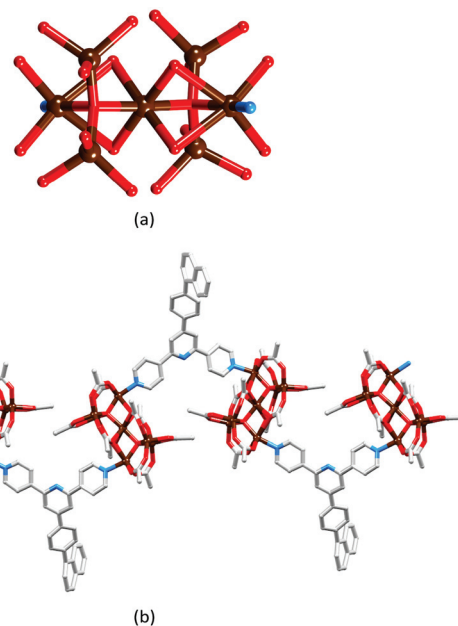**Fig. 13** (a) The $\{Zn_7O_{22}\}$ core of the $\{Zn_7(\mu\text{-OAc})_{10}(\mu_4\text{-O})_2\}$ node showing sites in which N-donors (blue) bind, and (b) part of the homo-chiral polymer chain in $2[\{Zn_7(\mu\text{-OAc})_{10}(\mu_4\text{-O})_2(4'\text{-}(naphthalen\text{-}1\text{-yl})\text{-}phenyl\text{-}4,2':6',4''\text{-tpy})\}_n]\cdot CH_2Cl_2$.

often built up along a crystallographic screw axis. The pitch of the helical chains is variable and the factors that control this and the homo- or heterochiral packing of helical chains has

been discussed. Introducing extended aryl domains in the 4′-position facilitates the formation of metallohexacycles when 4′-(arene)-4,2′:6′,4″-tpy ligands react with $ZnCl_2$ or $ZnBr_2$. This preference over polymer formation appears to driven by the interlocking of metallocycles through π-stacking which produces robust tube-like structures in the crystal lattice. The large void space in these tubes equips them to act as host materials.

Switching to metal(II) acetates in place of halides results in $[Zn_2(\mu\text{-OAc})_4(4'\text{-X-4,2':6',4''-tpy})]_n$ coordination polymers being prevalent; the latter possess zigzag backbones and assemble into flat sheets which interact through π-stacking to give efficiently packed structures that are typically solvent free unless substituent X is relatively small. The tendency for metal acetate cluster formation leads to the assembly of a number of unexpected coordination polymers, several of which exhibit multiply-stranded chains which retain key elements of the packing characteristics of the single-stranded $[Zn_2(\mu\text{-OAc})_4(4'\text{-X-4,2':6',4''-tpy})]_n$.

Acknowledgements

Notes and references

1 E. C. Constable and C. E. Housecroft, *Comprehensive Inorganic Chemistry II*, ed. J. Reedijk and K. R. Poeppelmeier, Elsevier, Oxford, 2013, vol. 8, p. 1.

2 S. J. Garibay, J. R. Stork and S. M. Cohen, *Prog. Inorg. Chem.*, 2009, **56**, 335.

3 G. Kumar and R. Gupta, *Chem. Soc. Rev.*, 2013, **42**, 9403.

4 E. C. Constable, *Coord. Chem. Rev.*, 2008, **252**, 842.

5 M. C. Das, S. Xiang, Z. Zhang and B. Chen, *Angew. Chem., Int. Ed.*, 2011, **50**, 10510.

6 See for example: R. Robson, *Dalton Trans.*, 2008, 5113.

7 M. Eddaoudi, D. B. Moler, H. Li, B. Chen, T. M. Reineke, M. O'Keeffe and O. M. Yaghi, *Acc. Chem. Res.*, 2001, **34**, 319.

8 See for example: K. Biradha, A. Ramanan and J. J. Vittal, *Cryst. Growth Des.*, 2009, **9**, 2969; S. R. Batten, N. R. Champness, X.-M. Chen, J. Garcia-Martinez, S. Kitagawa, L. Öhrström, M. O'Keeffe, M. P. Suh and J. Reedijk, *CrystEngComm*, 2012, **14**, 3001.

9 R. P. Thummel, *Comprehensive Coordination Chemistry II*, ed. J. A. McCleverty and T. J. Meyer, Elsevier, Oxford, 2003, vol. 1, p. 41.

10 E. C. Constable, *Chimia*, 2013, **67**, 388.

11 E. C. Constable, *Chem. Soc. Rev.*, 2007, **36**, 246.

12 M. Barquín, J. Cancela, M. J. González Garmendia, J. Quintanilla and U. Amador, *Polyhedron*, 1998, **17**, 2373.

13 F. H. Allen, *Acta Crystallogr., Sect. B: Struct. Sci.*, 2002, **58**, 380.

14 J. Bruno, J. C. Cole, P. R. Edgington, M. Kessler, C. F. Macrae, P. McCabe, J. Pearson and R. Taylor, *Acta Crystallogr., Sect. B: Struct. Sci.*, 2002, **58**, 389.

15 D. J. Tranchemontagne, J. L. Mendoza-Cortés, M. O'Keeffe and O. M. Yaghi, *Chem. Soc. Rev.*, 2009, **38**, 1257.

16 S. I. Vagin, A. K. Ott and B. Rieger, *Chem. Ing. Tech.*, 2007, **79**, 767.

17 M. Köberl, M. Cokoja, W. A. Herrmann and F. E. Kühn, *Dalton Trans.*, 2011, **40**, 6834.

18 L. Hou and D. Li, *Inorg. Chem. Commun.*, 2005, **8**, 190.

19 X.-Z. Li, M. Li, Z. Li, J.-Z. Hou, X.-C. Huang and D. Li, *Angew. Chem., Int. Ed.*, 2008, **47**, 6371.

20 G. W. V. Cave and C. L. Raston, *J. Supramol. Chem.*, 2002, **2**, 317.

21 E. C. Constable, G. Zhang, C. E. Housecroft and J. A. Zampese, *CrystEngComm*, 2011, **13**, 6864.

22 J. Heine, J. S. auf der Gunne and S. Dehnen, *J. Am. Chem. Soc.*, 2011, **133**, 10018.

23 B.-C. Wang, Q.-R. Wu, H.-M. Hu, X.-L. Chen, Z.-H. Yang, Y.-Q. Shangguan, M.-L. Yang and G.-L. Xue, *CrystEngComm*, 2010, **12**, 485.

24 E. C. Constable, G. Zhang, C. E. Housecroft, M. Neuburger and J. A. Zampese, *CrystEngComm*, 2010, **12**, 2146.

25 E. C. Constable, C. E. Housecroft, J. Schönle, S. Vujovic and J. A. Zampese, *Polyhedron*, 2013, **62**, 260.

26 E. C. Constable, C. E. Housecroft, P. Kopecky, M. Neuburger, J. A. Zampese and G. Zhang, *CrystEngComm*, 2012, **14**, 446.

27 See for example and references therein: P. Larpent, A. Jouaiti, N. Kyritsakas and M. W. Hosseini, *Dalton Trans.*, 2014, **43**, 2000; N. Marets, V. Bulach and M. W. Hosseini, *New J. Chem.*, 2013, **37**, 3549; A. Jouaiti, M. W. Hosseini, N. Kyritsakas, P. Grosshans and J.-M. Planeix, *Chem. Commun.*, 2006, 3078; W.-G. Lu, J.-Z. Gu, L. Jiang, M.-Y. Tan and T.-B. Lu, *Cryst. Growth Des.*, 2008, **8**, 192; S.-L. Cai, S.-R. Zheng, Z.-Z. Wen, J. Fan and W.-G. Zhang, *Cryst. Growth Des.*, 2012, **12**, 2355; L. Jiang, X.-L. Feng, C.-Y. Su, X.-M. Chen and T.-B. Lu, *Inorg. Chem.*, 2007, **46**, 2637; E.-Q. Gao, Y.-F. Yue, S.-Q. Bai, Z. He and C.-H. Yan, *J. Am. Chem. Soc.*, 2004, **126**, 1419.

28 E. C. Constable, C. E. Housecroft, S. Vujovic and J. A. Zampese, *CrystEngComm*, 2014, **16**, 328.

29 G. R. Newkome, T. J. Cho, C. N. Moorefield, R. Cush, P. S. Russo, L. A. Godínez, M. J. Saunders and P. Mohapatra, *Chem.–Eur. J.*, 2002, **8**, 2946.

30 E. C. Constable, G. Zhang, E. Coronado, C. E. Housecroft and M. Neuburger, *CrystEngComm*, 2010, **12**, 2139.

31 E. C. Constable, C. E. Housecroft, M. Neuburger, J. Schönle, S. Vujovic and J. A. Zampese, *Polyhedron*, 2013, **62**, 120.

32 E. C. Constable, C. E. Housecroft, S. Vujovic, J. A. Zampese, A. Crochet and S. R. Batten, *CrystEngComm*, 2013, **15**, 10068.

33 E. C. Constable, G. Zhang, C. E. Housecroft and J. A. Zampese, *Inorg. Chem. Commun.*, 2012, **15**, 113.

34 M.-C. Suen, Z.-K. Chan, J.-D. Chen, J.-C. Wang and C.-H. Hung, *Polyhedron*, 2006, **25**, 2325; M. T. Ng, T. C. Deivaraj and J. J. Vittal, *Inorg. Chim. Acta*, 2003, **348**, 173; J. Granifo, M. T. Garland and R. F. Baggio, *Polyhedron*, 2006, **25**, 2277; M. Kroger, C. Folli, O. Walter and M. Doring, *Adv. Synth. Catal.*, 2006, **348**, 1908.